JOURNAL OF BACTERIOLOGY, July 2006, p. 5045–5054 Vol. 188, No. 14
0021-9193/06/$08.00+0 doi:10.1128/JB.00128-06

Biochemical and Molecular Characterization of a Na^+-Translocating F_1F_o-ATPase from the Thermoalkaliphilic Bacterium *Clostridium paradoxum*†

Scott A. Ferguson, Stefanie Keis, and Gregory M. Cook*

Department of Microbiology and Immunology, Otago School of Medical Sciences, University of Otago, Dunedin, New Zealand

Received 23 January 2006/Accepted 19 April 2006

***Clostridium paradoxum* is an anaerobic thermoalkaliphilic bacterium that grows rapidly at pH 9.8 and 56°C. Under these conditions, growth is sensitive to the F-type ATP synthase inhibitor *N*,*N*′-dicyclohexylcarbodiimide (DCCD), suggesting an important role for this enzyme in the physiology of *C. paradoxum*. The ATP synthase was characterized at the biochemical and molecular levels. The purified enzyme (30-fold purification) displayed the typical subunit pattern for an F_1F_o-ATP synthase but also included the presence of a stable oligomeric *c*-ring that could be dissociated by trichloroacetic acid treatment into its monomeric *c* subunits. The purified ATPase was stimulated by sodium ions, and sodium provided protection against inhibition by DCCD that was pH dependent. ATP synthesis in inverted membrane vesicles was driven by an artificially imposed chemical gradient of sodium ions in the presence of a transmembrane electrical potential that was sensitive to monensin. Cloning and sequencing of the *atp* operon revealed the presence of a sodium-binding motif in the membrane-bound *c* subunit (viz., Q^{28}, E^{61}, and S^{62}). On the basis of these properties, the F_1F_o-ATP synthase of *C. paradoxum* is a sodium-translocating ATPase that is used to generate an electrochemical gradient of Na^+ that could be used to drive other membrane-bound bioenergetic processes (e.g., solute transport or flagellar rotation). In support of this proposal are the low rates of ATP synthesis catalyzed by the enzyme and the lack of the C-terminal region of the ε subunit that has been shown to be essential for coupled ATP synthesis.**

The membrane-bound bacterial F_1F_o-ATP synthase catalyzes ATP synthesis by utilizing the electrochemical gradient of protons, or in some instances Na^+ ions, to generate ATP from ADP and P_i (10, 48). The enzyme is also capable of working as an ATPase, hydrolyzing ATP to pump protons (or Na^+ ions) from the cytoplasm to the outside of the cell. On the basis of these properties, the F_1F_o-ATP synthase can be considered an assemblage of two separate molecular motors (F_1 and F_o) connected by a central stalk. Each motor operates with a unique function, depending upon the physiological conditions that exist within the cell for any given instance. The F_o motor, fuelled by the electrochemical gradient of protons ($\Delta\mu H^+$), operates under conditions of high $\Delta\mu H^+$ and low intracellular ATP. The transmembrane electrical potential ($\Delta\psi$) component of the $\Delta\mu H^+$ is obligatory in the process of ATP synthesis (10). The F_1 catalytic motor is fuelled by ATP and dominates under conditions of high intracellular ATP and an overall low $\Delta\mu H^+$. An important consequence of ATP hydrolysis by F_1 is the pumping of protons (or Na^+ ions) across the cytoplasmic membrane, thus establishing or adding to the overall $\Delta\psi$. This is a vitally important process in glycolytic anaerobic bacteria that lack a proton-translocating respiratory chain to generate the $\Delta\mu H^+$. In some cases, proton-pumping activity is coupled tightly to intracellular pH homeostasis (6). How the enzyme senses intracellular acidification is unknown.

The F_1F_o-ATP synthases studied in alkaliphilic bacteria highlight an interesting contrast in ATPase function and regulation. The alkaliphilic bacteria are a unique group of organisms that thrive at high external pH values (pH 8.5 to 11.5) yet maintain their cytoplasmic pH near neutral (pH 8.0). These unique growth conditions result in a well-established bioenergetic problem (28). As the $\Delta\mu H^+$ is the sum of the $\Delta\psi$ and the pH gradient (ΔpH), the low $\Delta\mu H^+$ observed in the alkaliphilic bacteria is due to the inverted pH gradient (alkaline outside, acidic inside) and not to a low $\Delta\psi$ as is the case for anaerobes (9). The low $\Delta\mu H^+$ observed in alkaliphilic bacteria is considered suboptimal for proton-coupled bioenergetic processes (e.g., solute transport, motility, and ATP synthesis) (9, 28). However, in all alkaliphilic bacteria examined to date, the F_1F_o-ATP synthase remains exclusively coupled to protons (4, 14, 15), and several models have been put forward to account for proton-coupled ATP synthesis in alkaliphilic bacteria (27). For solute transport and motility, aerobic alkaliphiles use sodium in combination with the $\Delta\psi$ as the coupling ion and not protons (28, 43).

While our understanding of the F_1F_o-ATP synthase's mode of operation in aerobic alkaliphiles is expanding, there have been no detailed biochemical or molecular studies conducted on the F_1F_o-ATP synthases from anaerobic alkaliphiles. *Clostridium paradoxum* is a ubiquitous gram-positive, spore-forming rod found in sewage sludge and represents the most thermoalkaliphilic anaerobic organism studied to date (34). Optimal growth conditions are at pH 9.8 and 56°C, but *C. paradoxum* is capable of growth over the pH range 6.9 to 10.3 (5), and based on these properties it is best characterized as a facultative alkaliphile. Under optimal growth conditions, *C. paradoxum* generates a $\Delta\psi$ of approximately −90 mV, but the

* Corresponding author. Mailing address: Department of Microbiology and Immunology, University of Otago, P.O. Box 56, Dunedin, New Zealand. Phone: 64 3 4797722. Fax: 64 3 4798540. E-mail: greg.cook@stonebow.otago.ac.nz.

† This paper is dedicated to Professor Peter Dimroth on the occasion of his 65th birthday.

total $\Delta\mu H^+$ is only −25 mV due to an inverted pH gradient (acidic inside) (5). Despite this very low $\Delta\mu H^+$, *C. paradoxum* grows at a doubling time of 16 min (5, 34).

In this communication we report on the biochemical and molecular characterization of the first sodium-translocating F_1F_o-ATPase from an alkaliphilic bacterium and discuss the role of this enzyme in the physiology of anaerobic growth at high pH and temperature.

MATERIALS AND METHODS

Abbreviations. The following abbreviations are used in this paper: IPTG, isopropyl-β-D-thiogalactopyranoside; X-Gal, 5-bromo-4-chloro-3-indolyl-β-D-galactopyranoside; P_i, inorganic phosphate; MOPS, 4-morpholinepropanesulfonic acid; DTT, dithiothreitol; PEG 6000, polyethylene glycol 6000; SDS-PAGE, sodium dodecyl sulfate-polyacrylamide gel electrophoresis; TCA, trichloroacetic acid; OD_{600}, optical density at 600 nm; MES, morpholinoethanesulfonic acid; ACMA, 9-amino-6-chloro-2-methoxyacridine; AO, acridine orange; DCCD, *N,N′*-dicyclohexylcarbodiimide; TE, Tris-EDTA; DDM, *n*-dodecyl-β-D-maltoside; OG, *n*-octyl-β-D-glucopyranoside; CCCP, carbonyl cyanide *m*-chlorophenylhydrazone.

Bacterial strains, plasmids, and culture conditions. *Clostridium paradoxum* DSM 7308 was maintained as a spore stock preparation in sterile distilled water at 4°C. Spores were germinated by heat shock at 75°C for 2 min, followed by rapid cooling on ice for 45 s. *C. paradoxum* was grown anaerobically at 56°C in YTG medium which contained, per liter, 5.3 g of Na_2CO_3, 0.36 g of $Na_2HPO_4 \cdot 2H_2O$, 0.075 g of KCl, 5 g of yeast extract, 10 g of tryptone, 0.2 g of cysteine HCl, 0.2 g of $Na_2S \cdot 9H_2O$, and 0.3% (wt/vol) glucose. The pH of the medium was adjusted to 10.1 at 25°C with 5 M NaOH, which is equivalent to pH 9.8 at 55°C. Bacterial growth was routinely monitored by following the OD_{600}. Where applicable, specific inhibitors of growth were dissolved in ethanol and added at early exponential phase. *Escherichia coli* DH10B (13) was used for all cloning experiments and was routinely grown at 37°C in 2× YT broth or Luria-Bertani (LB) agar. *E. coli* plasmids used for cloning were the low-copy vector pCL1921 (33) and pUC8 (59). Transformants of *E. coli* DH10B were selected on LB agar containing either spectinomycin at 100 μg/ml (pCL1921) or ampicillin at 100 μg/ml (pUC8). IPTG (24 μg/ml) and X-Gal (40 μg/ml) were included where appropriate.

Preparation of inverted membrane vesicles. Typically, 5 g of frozen cells from *C. paradoxum* were washed twice in 50 mM MOPS buffer (pH 7.5) and the cells were then resuspended in 10 ml of membrane buffer (50 mM MOPS [pH 7.5], 2 mM $MgCl_2$, 0.1 mM phenylmethylsulfonyl fluoride, 1 mM DTT, and 10% [vol/vol] glycerol). The suspension was treated with 2 mg/ml lysozyme for 45 min at room temperature with constant stirring. DNase I (2 mg) and 15 mM (final concentration) $MgCl_2$ were added and mixed for a further 15 min. Unless otherwise stated, the following steps were performed at 4°C. Cells were disrupted by three passages through a precooled French pressure cell at 20,000 lb/in^2. Unbroken cell material was removed via low-speed centrifugation (8,000 × *g* for 15 min), and the membranes were collected by centrifugation at 180,000 × *g* for 45 min. Membranes were washed in the membrane buffer and centrifuged as described above. Washed membranes were resuspended in 1 ml of membrane buffer per gram of original cells used, to a protein concentration of 10 to 20 mg/ml.

Solubilization and purification of the F_1F_o-ATPase. Prior to solubilization, membranes were resuspended in membrane buffer containing 1% sodium cholate (final concentration) and were incubated for 1 h at room temperature with constant stirring. The suspension was centrifuged at 180,000 × *g* for 45 min to collect the ATPase-containing membranes. The supernatant after this wash step contained negligible F_1F_o-ATPase activity. For solubilization of the ATPase, the washed membrane pellet was resuspended in 5 to 10 ml of membrane buffer containing 1% Triton X-100, and after 1 h of incubation at room temperature with constant stirring, the insoluble material was removed by centrifugation at 180,000 × *g* for 45 min. The solubilized membrane proteins were supplemented with 50 mM $MgCl_2$, and contaminating proteins were precipitated with 4 to 6% PEG 6000 for 20 min as described by Laubinger and Dimroth (31). Precipitated proteins were removed by centrifugation at 39,000 × *g* for 20 min. To precipitate the ATPase, 10 to 12% (final concentration) PEG 6000 was added to the supernatant containing 90% of the ATPase activity. The precipitate was collected by centrifugation as described above, and the pellet was resuspended in 10 mM Tris-Cl (pH 8.0) containing 2 mM $MgCl_2$ to a protein concentration of about 1.5 mg/ml. Further insoluble material was removed by a third centrifugation. The ATPase-containing supernatant was immediately frozen at −80°C, where it remained stable for at least 2 months.

Proteins were routinely analyzed by 14% SDS-PAGE using the buffer system described by Laemmli (29). Polypeptide bands were visualized by silver staining (40). Samples treated with TCA were not heated prior to SDS-PAGE. Protein concentrations were determined using a bicinchoninic acid protein assay kit (Sigma) with bovine serum albumin as the standard.

Purification and dissociation of the *c*-oligomer. The *c*-oligomer was isolated from the PEG-purified ATPase by the procedure established by Meier et al. (38). Briefly, the ATPase was dissociated in 1% *N*-lauroylsarcosine and heated to 65°C for 10 min, followed by ammonium sulfate precipitation of all ATPase subunits except the *c*-oligomer. Dissociation of the *c*-oligomer into monomeric units was carried out by acidification with TCA as described by Matthey et al. (36).

Reconstitution of the purified F_1F_o-ATPase. A suspension of 30 mg phosphotidylcholine (type II S; Sigma) was suspended in 1 ml of 10 mM Tricine-KOH (pH 8.0), 2 mM $MgCl_2$, and 1 mM DTT. To prepare the lipids for reconstitution, the solution was sonicated twice for 30 s on ice with a tip sonicator at an output of 40 W and cooled on ice for 1 h. Purified ATPase was added to the suspension to obtain a protein-to-lipid ratio of 50 to 200:1 (wt/wt). The detergent/lipid ratio was optimized by titrating the liposomes with Triton X-100, and the solubilization was followed at OD_{540}, similar to the method employed by Knol et al. (25). We utilized 0.4% Triton X-100, a concentration known to favor insertion of the ATPase with F_1 facing outwards. The mix was left on ice for 20 min and then was gently mixed for 45 min at room temperature. After this time the Triton X-100 was removed slowly via adsorption to Bio-Beads (Bio-Rad). Consecutive aliquots of 50 mg, 50 mg, and 80 mg of beads were added for 1 h each with continuous mixing at room temperature. The proteoliposomes were collected by ultracentrifugation in an SW60 (Beckman) rotor at 180,000 × *g* for 1 h, the supernatant was removed, and the pellet was resuspended in 10 mM Tricine-KOH (pH 8.0) and 2 mM $MgCl_2$ buffer. Under these conditions, greater than 70% of the ATPase was incorporated into the proteoliposomes with F_1 accessible as determined by ATP hydrolysis assays. Proteoliposomes were utilized immediately for either ATP hydrolysis or ATP synthesis determination. The concentration of Na^+ associated with the proteoliposomes or a sample of interest was measured by atomic absorption at 588.9 nm with a Shimadzu AA646 atomic absorption-flame emission spectrophotometer. The contaminating concentration of Na^+ was between 20 and 40 μM for all experiments where precautions were taken to specifically remove sodium.

ATP hydrolysis determination and ATP synthesis measurements. ATP hydrolysis activity from inverted membranes or the purified ATPase was measured using the spectrophotometric ATP-regenerating assay at 40°C. The standard assay mix (final volume, 1 ml) contained 50 mM MOPS (pH 7.5), 2 mM $MgCl_2$, 3 mM phospho(enol)pyruvate, 0.3 mM NADH, 3.2 U/ml lactate dehydrogenase, and 0.57 U/ml pyruvate kinase. The reaction was initiated by the addition of 4 mM (final concentration) disodium-ATP, and the rate of NADH oxidation was followed continuously at 340 nm with a Cary 50 (Varian) spectrophotometer. The pH profile of the ATPase was characterized in a three-buffer mix composed of 50 mM MES–MOPS–Tris-Cl. To reduce the amount of sodium present, when required, purified ATPase was dialyzed overnight at 4°C against 10 mM Tris-Cl (pH 8.0) and 2 mM $MgCl_2$. For sodium-free measurements, disodium-ATP was replaced with Tris-ATP (Sigma). Under conditions where the ATP-regenerating assay could not be used, ATP hydrolysis was monitored via the release of P_i (26). The assay solution contained 50 mM MOPS (pH 7.5), 2 mM $MgCl_2$, and 4 mM disodium-ATP. The amount of nonspecific P_i released during the assay was corrected for, and the linearity of the assay was confirmed over time. One unit of ATPase activity was defined as the amount of enzyme that liberated 1 μmol of P_i or ADP per min at 40°C. For all experiments, the values reported are the means from at least three separate experiments and the experimental error associated with these values was less than 15%.

ATP synthesis in inverted membrane vesicles was determined via the standard luciferin-luciferase system, monitoring the light emitted with a chemiluminometer (FB 12 luminometer; Berthold). The ATP synthesis reactions were carried out at 40°C in a 400-μl volume containing 10 μl of inverted membrane vesicles (K^+_{in} = 5 mM), 10 mM Tricine-KOH (pH 8.0), 2 mM $MgCl_2$, 5 mM KH_2PO_4, 2.5 mM ADP, and 200 mM KCl. The synthesis reaction was initiated via the addition of 2 μM valinomycin to induce a potassium diffusion potential of approximately 100 mV as calculated using the Nernst equation: $61 \times \log_{10}([K^+]_{out}/[K^+]_{in})$. To load inverted membrane vesicles with Na^+, vesicles were incubated in 50 mM MOPS (pH 7.5) buffer containing 100 mM NaCl overnight at 4°C. To create a chemical gradient of sodium ions (ΔpNa^+) of 100 mV $\{61 \times \log_{10}([Na^+]_{out}/[Na^+]_{in}\}$, Na^+(100 mM)-loaded vesicles were diluted 40-fold into 10 mM Tricine-KOH (pH 8.0), 2 mM $MgCl_2$, 5 mM KH_2PO_4, and 2.5 mM ADP. To additionally impose a $\Delta\psi$ (100 mV) in the presence of ΔpNa^+, 200 mM KCl

and valinomycin were included in the dilution buffer. Samples (50 μl) were withdrawn every 10 to 20 s, and the reaction was stopped by diluting the sample with 400 μl of stop mix containing 50 mM MOPS supplemented with 1% TCA and 2 mM EDTA. Samples were diluted 10-fold, and the luciferase reaction was initiated by adding 25 μl of luciferin-luciferase mix to 50 μl of diluted sample in 400 μl of synthesis buffer (50 mM Tris-acetate [pH 7.8], 2 mM EDTA, 50 mM $MgCl_2$).

To examine proton-pumping activity of the reconstituted ATPase in proteoliposomes or inverted membrane vesicles, ATP-dependent quenching was monitored with two fluorescent probes, ACMA (Sigma) or AO (Kodak). Typically, assays were conducted in a 3-ml cuvette containing a weak buffer (i.e., 5 mM potassium phosphate [pH 7.5], 1 μM ACMA or AO, and 2 mM $MgCl_2$), and quenching was examined at 40°C. The reaction was initiated via the addition of 1 mM Tris-ATP once the fluorescence signal had stabilized. Fluorescence was measured at an excitation wavelength of 410 nm or 492 nm and an emission wavelength of 480 nm or 528 nm (slit width, 10 nm) for ACMA or AO, respectively, in a Cary Eclipse fluorescence spectrophotometer.

Purified F_1F_o-ATPase inhibition by DCCD. ATPase (25 μg) inhibition by DCCD was conducted as described previously by Kluge and Dimroth (24). Samples were incubated at 25°C with the appropriate concentration of DCCD (or equivalent concentration of ethanol) in a total volume of 0.1 ml. Samples of 20 μl were taken at the times indicated and diluted into 1 ml of ATPase assay mixture, and residual ATPase activity was determined.

DNA preparation and manipulation. Chromosomal DNA from *C. paradoxum* was extracted from cultures grown to an OD_{600} of 0.3 to 0.4. Cells were harvested by centrifugation, washed with TE (5:2) buffer (50 mM Tris-Cl, 20 mM EDTA, pH 8.0) containing 0.5 M NaCl, washed in TE (5:2) buffer, and resuspended in TE (5:2) buffer containing 500 μg/ml lysozyme and 200 μg/ml RNase A. The suspension was incubated at 37°C for 30 min before the addition of 10 mg/ml *N*-lauroylsarcosine and 200 μg/ml proteinase K. The suspension was incubated at 50°C for 18 h. All of the above steps were carried out in an anaerobic glove box (Forma Scientific, Inc.). Genomic DNA was subsequently isolated by standard phenol-chloroform extraction and precipitation with ethanol. PCR products for probing and sequencing were purified with the High Pure PCR purification kit (Roche). Gel electrophoresis of restriction fragments, plasmids, or PCR products was carried out in agarose gels. DNA in agarose gels was transferred onto Hybond-N^+ nylon membranes (Amersham) using a VacuGene (Pharmacia-LKB) vacuum-blotting system as described previously (23). DNA was labeled with [α-^{32}P]dCTP (Amersham) by random priming using Ready-to-Go DNA labeling beads (Amersham). Prehybridization and hybridization were carried out in the same hybridization buffer (2) at 65°C for 18 to 24 h, and membranes were washed stringently as described previously (23) before exposure to X-ray film (Agfa). Plasmid DNA was isolated with either a QIAGEN plasmid midi kit (QIAGEN) or the High Pure plasmid isolation kit (Roche). DNA from agarose gels was extracted using the QiaexII gel extraction kit (QIAGEN). Restriction enzymes, DNA ligase, and alkaline phosphatase were purchased from Roche and used as specified by the manufacturer.

PCR and cloning of *atp* operon. A 506-bp PCR product was amplified using *C. paradoxum* genomic DNA as the template and primers atpDfwd (5′-CAAATG AATGAGCCGCCTGG-3′) and atpDrev (5′-CGATGATATCTTGAAGTTC-3′), which are derived from highly conserved regions of DNA sequence in the *atpD* genes coding for the β subunits of *Moorella thermoacetica* (formerly *Clostridium thermoaceticum*) (accession number U64318), *Clostridium acetobutylicum* (accession number AF101055), *Clostridium pasteurianum* (accession number AF283808), and *Clostridium perfringens* (accession number NC_003366). PCR was carried out using the Expand high-fidelity PCR system (Roche), and amplification was achieved using the program outlined previously (23). Using this 506-bp PCR product as a probe, an approximately 12-kb ClaI fragment was identified in digests of genomic DNA from *C. paradoxum*. This 12-kb ClaI fragment was cloned into the AccI-digested vector pCL1921 to form recombinant plasmid pA9. To facilitate sequencing of the *atp* operon, four HindIII fragments of 3 kb, 2.2 kb, 1.6 kb, and 1.5 kb from pA9 were subcloned into pUC8 to yield subclones pFrag2, pFrag3, pFrag5, and pFrag4, respectively.

DNA sequencing and analysis. DNA sequencing was carried out using a BigDye terminator cycle sequencing ready reaction sequencing kit (Applied Biosystems) and a model ABI3730 automated DNA sequencer (Applied Biosystems). The sequence of the *atp* operon was determined in both strands, and contigs were assembled using the SeqMan program (DNASTAR Inc.). Homology searches of nonredundant databases at the National Center for Biotechnology Information, using BLASTX and BLASTN, were done through the WWW BLAST server (www.ncbi.nlm.nih.gov).

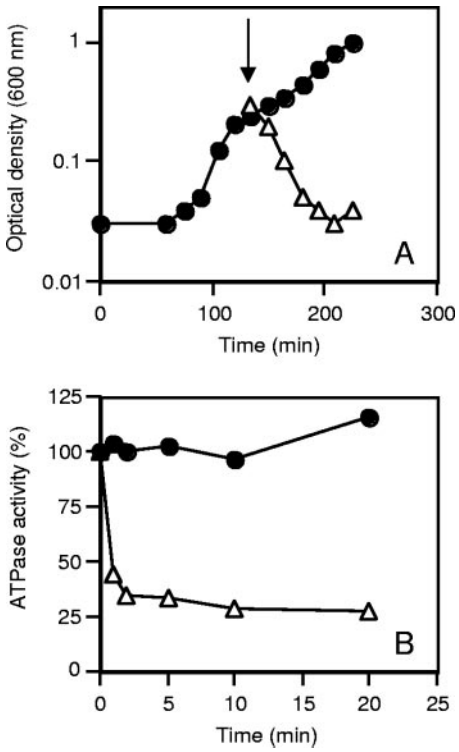

FIG. 1. Inhibition of growth and ATP hydrolysis activity of inverted membrane vesicles by DCCD. (A) Growth of *C. paradoxum* in the presence of 50 μM DCCD (△) or tetrachlorosalicylanilide (20 μM) or an equivalent volume of ethanol (●). The arrow indicates addition of inhibitor or ethanol at mid-exponential growth phase. (B) Inverted membrane vesicles (100 μg of protein) were incubated in 0.1 ml of buffer containing 50 mM MOPS-KOH, pH 7.5, at 25°C in the presence of 200 μM DCCD (△) or an equal volume of absolute ethanol (●). Samples (20 μl) were taken at the times indicated, and the amount of ATPase activity was determined via the ATP-regenerating assay.

Nucleotide sequence accession number. The DNA sequence of the *C. paradoxum atp* operon has been submitted to the GenBank database under accession number DQ193538.

RESULTS

***C. paradoxum* harbors a DCCD-sensitive F-type ATPase.** Growth of *C. paradoxum* with glucose as the carbon and energy source was inhibited by the F-type ATPase inhibitor DCCD (Fig. 1A). No inhibition of growth was observed with either an equivalent volume of ethanol or the protonophore tetrachlorosalicylanilide (Fig. 1A). To validate these observations, we prepared inverted membrane vesicles of *C. paradoxum* and examined the effect of DCCD on ATP hydrolysis activity (Fig. 1B). High levels of ATP hydrolysis activity were detected in inverted membrane vesicles, with a specific activity of 0.5 U/mg of protein at 40°C (Table 1). ATPase activity was inhibited by >70% after 20 min of incubation with DCCD (200 μM) (Fig. 1B), suggesting that *C. paradoxum* harbors an F-type ATPase.

Purification and subunit composition of the F_1F_o-ATP synthase from *C. paradoxum*. In order to characterize the ATPase, we proceeded to isolate the enzyme in a pure form. Initial experiments indicated that if a 1% sodium cholate wash of inverted membrane vesicles was performed before solubiliza-

TABLE 1. Purification of the F_1F_o-ATPase from *C. paradoxum*[a]

Step	Protein (mg)	Activity (U)[b]	Sp act (U/mg)	Purification (fold)	Yield (%)
Membrane vesicles	53.0	27.0	0.5	1.0	100.0
Cholate-washed vesicles	24.0	26.0	1.1	2.2	96.0
Triton X-100 (1%) solubilization	8.0	47.0	6.0	12.0	174.0
PEG 6000 precipitation	1.5	22.0	15.0	30.0	81.0

[a] The starting material consisted of 5 g (wet weight) of cells, and the results represent averages for three preparations.
[b] ATPase activity was measured by the ATP regenerating assay, and one ATPase unit is equivalent to 1 μmol of ADP produced/min at 40°C.

tion, this greatly improved the yield and purity of the ATPase. Importantly, the sodium cholate wash resulted in no significant loss of ATPase activity but was successful in reducing the amount of protein associated with the membranes by about 50%, yielding a 2.2-fold increase in specific ATPase activity (1.1 U/mg of protein) (Table 1). Triton X-100 solubilization of the cholate-washed membranes led to an apparent doubling in the total number of ATPase units (i.e., from 26 to 47), but this was due to an activation of the enzyme by this detergent. The overall solubilization process resulted in a 12-fold purification of the enzyme (Table 1). Other detergents (viz., DDM and OG) were examined for their ability to solubilize the ATPase. While DDM proved more effective at solubilizing the ATPase than either OG or Triton X-100 (data not shown), the PEG 6000 fractionation proved unsuccessful with the ATPase in this detergent. Typical data for ATPase purification from 5 g of cells are summarized in Table 1, and the values reported are averages from three separate enzyme purifications. The protocol resulted in a 30-fold purification of the enzyme, with a final specific activity of 15 U/mg of protein. SDS-PAGE of the enzyme (Fig. 2A, lane 1) displayed the distinctive subunit migration profile for an F-type ATPase, with five F_1 subunits (α, β, γ, δ, and ε) and three F_o subunits (*a*, *b*, and *c*). Several contaminating polypeptides are observed in our purified ATPase preparation, migrating at approximately 35 kDa, 40 kDa, and 50 kDa. These polypeptides could not be removed by anion-exchange chromatography.

SDS-PAGE revealed a protein running at an apparent molecular mass of 60 kDa (Fig. 2A, lane 1). TCA treatment, a procedure known to dissociate *c*-oligomers (36, 41), resulted in the disappearance of this 60-kDa protein and the appearance of a protein at 8.2 kDa, the size attributed to the monomeric *c* subunit (Fig. 2A, lane 2). The oligomeric *c*-ring was isolated from the purified ATPase, and all of the monomeric form could be obtained by treatment with TCA, which is indicative of a stable oligomeric *c*-ring in *C. paradoxum* (Fig. 2B, compare lanes 1 and 2).

Biochemical properties of the purified ATPase from *C. paradoxum*. The properties of the purified F_1F_o-ATP synthase, unless otherwise stated, were examined using the ATP-regenerating assay at 40°C in 50 mM MOPS buffer (pH 7.5). The enzyme displayed a temperature profile typical for a thermophilic enzyme, with a temperature optimum of 50°C, closely reflecting the growth optimum of this organism (Fig. 3A). The pH optimum of the purified enzyme was broad, with high levels of activity over the pH range from 7.6 to 8.5 (Fig. 3B). Remarkably, the enzyme still retained about 20% of its maximum activity at below pH 7.0 (Fig. 3B). As is typical of an F-type ATPase, ATP hydrolysis activity was dependent upon the presence of the divalent cation $MgCl_2$, with an apparent K_m of 1 mM (Fig. 3C). $CaCl_2$ could function in place of $MgCl_2$, although the affinity was much lower (Fig. 3D). The purified enzyme had an apparent K_m for ATP of 0.55 mM when the Mg^{2+}/ATP ratio was maintained at 2:1 (Fig. 3E). In membrane vesicles, ATPase activity at 4°C appeared to be stable, retaining near 100% of the starting activity for a period extending beyond 4 days (Fig. 3F). This was in contrast to the enzyme in its purified form, which rapidly lost activity overnight and retained only about 25% of its starting activity after 5 days of storage at 4°C (Fig. 3F).

The F_1F_o-ATP synthase from *C. paradoxum* is rapidly inhibited by DCCD in a pH-dependent manner, and DCCD inhibition can be prevented via the addition of Na^+. It has been reported that ATPases capable of translocating Na^+ ions show a specific stimulation of their ATP hydrolysis activity in the presence of low concentrations of NaCl (30, 41, 46). ATPase activity of the purified *C. paradoxum* enzyme was stimulated three- to fourfold (pH 7.0) or five- to sixfold (pH 9.0) with increasing concentrations of Na^+ (Fig. 4). Kinetic analyses of the data in Fig. 4, using the Lineweaver-Burk equation, indicated that the apparent K_m for Na^+ at pH 7.0 and 9.0 was 0.5 mM (data not shown).

A characteristic property of F-type ATPases is their specific inhibition by DCCD (35). This inhibition is due to the binding of DCCD to a highly conserved carboxyl residue (E^{61}) in the *c*

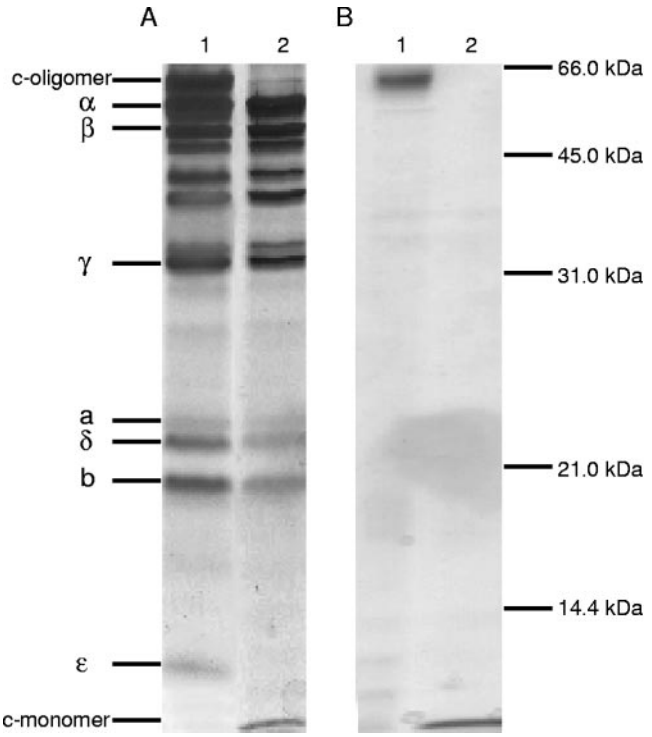

FIG. 2. Analysis of purified F_1F_o-ATPase and *c*-oligomer by SDS-PAGE. (A) Lane 1, 5 μg of purified F_1F_o-ATPase; lane 2, 5 μg of purified F_1F_o-ATPase treated with TCA, as described in Materials and Methods. (B) Lane 1, 1 μg of purified *c*-oligomer; lane 2, purified *c*-oligomer treated with TCA. Gels were stained with silver.

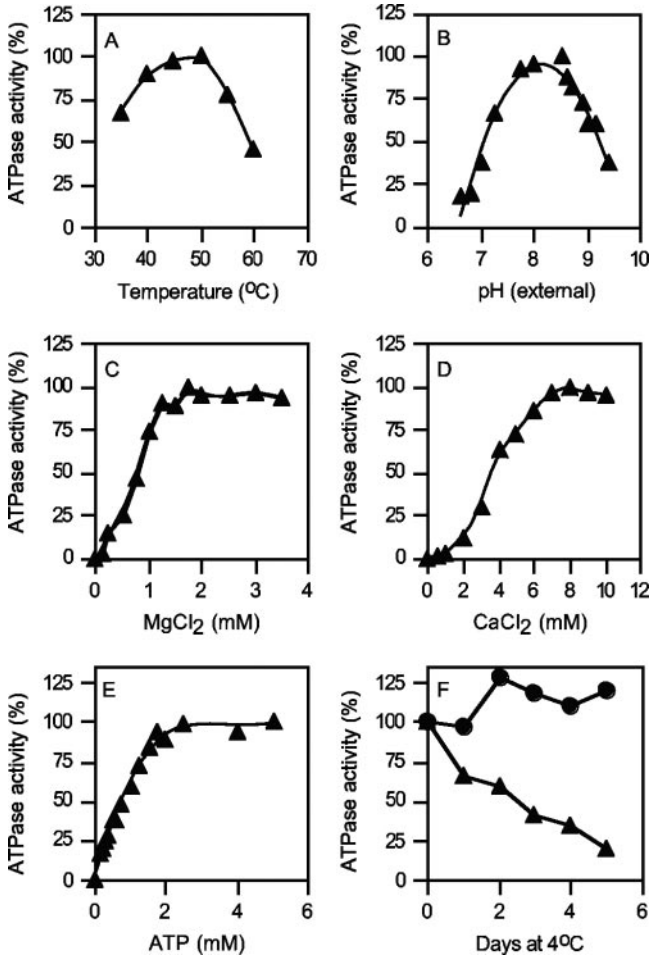

FIG. 3. Biochemical properties of the purified F_1F_o-ATPase. (A to E) Effects of temperature (A), extracellular pH (B), $MgCl_2$ (C), $CaCl_2$ (D), and ATP (E) on ATPase activity. (F) Stability of the purified enzyme (20 μg) (▲) in 10 mM Tris-Cl (pH 8.0) with 2 mM $MgCl_2$, compared to membrane vesicles (●) stored in membrane buffer at 4°C. ATPase activity was determined using the ATP-regenerating assay (B, E, and F) or by determination of P_i at 40°C (A, C, and D); 100% ATPase activity was in the range of 15 to 20 U/mg protein.

subunit that has been shown to be located in the center of the cytoplasmic membrane (11, 54). When the purified ATPase from *C. paradoxum* was incubated in the presence of increasing concentrations of DCCD for 5 min, it was observed that as little as 25 μM DCCD caused a 75% inhibition of ATPase activity (Fig. 5A). Incubation with 200 μM DCCD resulted in rapid inactivation of the ATPase within 5 min (Fig. 5B). We routinely used 200 μM DCCD to ensure strong inhibition of ATPase activity. The high level of DCCD inhibition indicated that the enzyme remained tightly coupled throughout the purification procedure.

Protection from DCCD inhibition in a pH-dependent manner by Na^+ ions has been observed with the ATP synthases from *Propionigenium modestum* (24), *Acetobacterium woodii* (51), and *Ilyobacter tartaricus* (38). When the ATPase from *C. paradoxum* was incubated at pH 7.0 in the presence of 200 μM DCCD and high levels of NaCl (50 mM), the inhibition of ATPase activity after 20 min was reduced to approximately

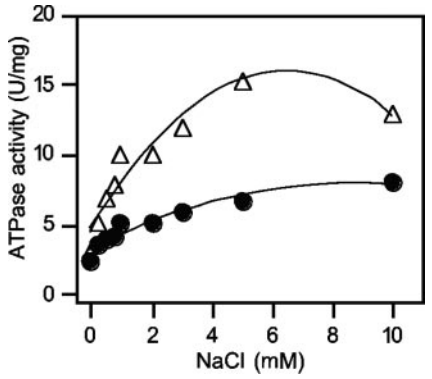

FIG. 4. Stimulation of the *C. paradoxum* F_1F_o-ATPase by NaCl. The ATPase was dialyzed overnight as described in Materials and Methods. Purified ATPase (10 μg) was used to determine the effect of increasing concentrations of Na^+ ions on ATPase activity. The ATPase assay mixture contained either 50 mM MOPS (pH 7.0) (●) or 50 mM Tricine-KOH (pH 9.0) (△), and the NaCl concentrations indicated.

40% of the original ATPase activity (Fig. 5C). In contrast, 1 mM NaCl offered no protection against the inhibitory effects of DCCD at pH 7.0 (Fig. 5C). At pH 9.0, the *C. paradoxum* ATPase retained about 25% of its activity after 20 min of DCCD treatment with no NaCl or low levels of NaCl (150 μM)

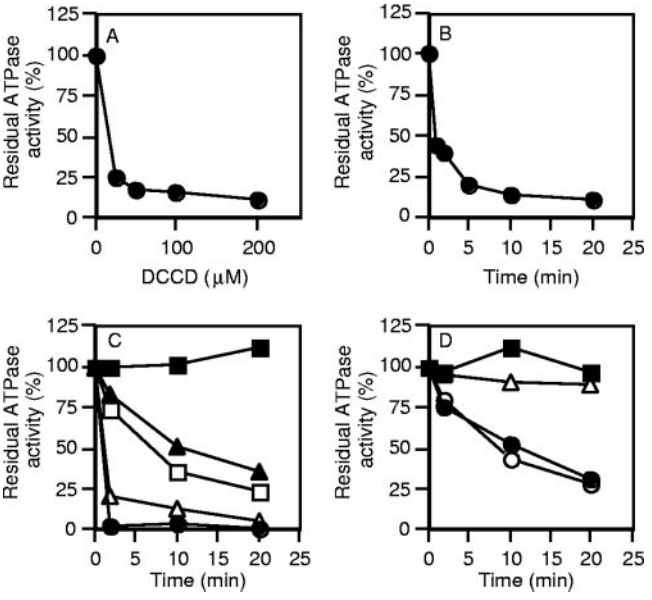

FIG. 5. Effect of NaCl on DCCD inhibition of the purified F_1F_o-ATPase. The purified ATPase (25 μg) was incubated at 25°C in 50 mM MOPS (pH 7.5) with increasing concentrations of DCCD for 20 min in the absence of NaCl (A) or in 50 mM MOPS (pH 7.5) and 200 μM DCCD (B). To examine the effect of pH and Na^+ ions on DCCD inhibition, the ATPase was incubated in 50 mM MOPS (pH 7.0) (C) or 50 mM Tricine-KOH (pH 9.0) in the presence of 200 μM DCCD (D). The following additions of NaCl were made: none (●), 150 μM NaCl (○), 1 mM NaCl (△), 10 mM NaCl (□), or 50 mM NaCl (▲). The control sample in the presence of an equivalent amount of ethanol (0.2%) contained no NaCl and no DCCD (■). ATPase activity was determined as described in Materials and Methods; 100% ATPase activity was in the range of 15 to 20 U/mg protein.

(Fig. 5D). However, in the presence of 1 mM NaCl at pH 9.0, DCCD had no inhibitory effect (Fig. 5D).

ATP synthesis in inverted membrane vesicles can be driven by an artificially imposed ΔpNa^+ in the presence of $\Delta\psi$ that is sensitive to monensin. To study vectorial ion transport with the F_1F_o-ATPase of *C. paradoxum*, numerous attempts to reconstitute the ATPase into proteoliposomes were made. Despite successful reconstitution of the ATPase as evidenced by SDS-PAGE of proteoliposomes and the detection of ATP hydrolysis activity in proteoliposomes, no ATP-dependent proton pumping or ATP synthesis could be detected (data not shown). Several other reconstitution techniques were employed (e.g., cholate dialysis, OG dilution, and freeze-thawing with sonication), but all proved to be unsuccessful. Due to the failure to reconstitute the native enzyme, ATP synthesis and ATP-dependent proton pumping were examined in inverted membrane vesicles. A characteristic property of sodium-translocating F-ATPases from bacteria that grow at neutral pH is their specific inhibition of ATP-dependent proton pumping by Na^+ ions (32, 41). No ATP-dependent quenching (indicative of proton pumping) of the fluorescent signal (i.e., with either ACMA or AO) with *C. paradoxum* inverted membranes could be detected, even at a pH of 7.0 to facilitate the use of protons. We could, however, readily detect quenching with inverted membrane vesicles of *E. coli* (positive control) (data not shown).

ATP synthesis in inverted membrane vesicles was examined using a valinomycin-induced potassium diffusion potential. When a membrane potential ($\Delta\psi$) of 100 mV was applied, ATP synthesis proceeded at an initial rate of approximately 80 nmol of ATP/mg protein/min (Fig. 6A). No ATP synthesis was observed in the absence of valinomycin (i.e., no $\Delta\psi$ generated) (Fig. 6A). ATP synthesis in the presence of a $\Delta\psi$ was inhibited by either DCCD (50 μM) or CCCP (20 μM) (Fig. 6B). ATP synthesis could be driven by a ΔpNa^+ in the presence of a $\Delta\psi$ (i.e., valinomycin addition and high external K^+). ATP synthesis under these conditions was sensitive to the sodium ionophore monensin (5 μM) (Fig. 6C). CCCP (20 μM) completely abolished ATP synthesis in the absence of a ΔpNa^+, and this was restored to approximately 30% of the control value (Fig. 6C) if a ΔpNa^+ was present (Fig. 6D). The inhibitory effect of CCCP on ATP synthesis, even in the presence of a ΔpNa^+, most likely reflects the dissipation of the $\Delta\psi$ component by this compound.

Cloning, sequencing, and analysis of the *atp* operon of *C. paradoxum*. To identify the *C. paradoxum atp* operon, PCR was performed using primers derived from highly conserved regions of DNA sequence in the *atpD* genes (β subunit) of *Clostridium* species. This resulted in the amplification of a 506-bp PCR product, the sequence of which was highly homologous with those of β subunits from other bacterial F_1F_o-ATP synthases. This PCR product was subsequently used as a probe to anneal to *C. paradoxum* genomic DNA digested with various enzymes, and an approximately 12-kb ClaI fragment was identified. Since our aim was to clone the entire *atp* operon of *C. paradoxum*, this 12-kb ClaI fragment was cloned into the cloning vector pCL1921 to yield the recombinant plasmid pA9. Analysis of the DNA sequence from the 3′ end of the pA9 clone revealed that it was homologous to the *atpC* (ε subunit) of other previously sequenced *atpC* genes, confirming the presence of the entire *atp* operon in this clone. To aid in the sequencing of the *atp* operon, four HindIII fragments from pA9 were subcloned into pUC8. Three of the subclones contained genes homologous to *atp* genes from other bacteria, whereas the sequence from subclone pFrag3 had homology to proteins coding for undecaprenyl-phosphate α-*N*-acetylglucosaminyltransferases and UDP-*N*-acetylglucosamine 2-epimerases and was therefore not included for further study.

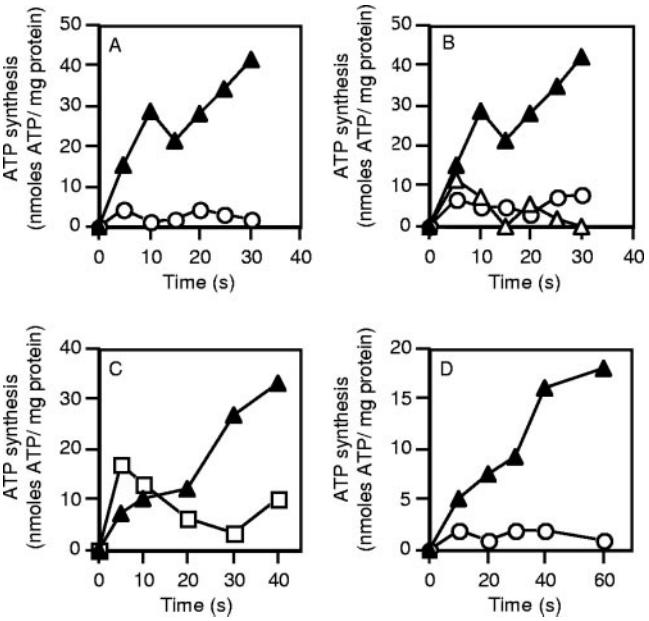

FIG. 6. ATP synthesis in *C. paradoxum* membrane vesicles. (A) ATP synthesis in inverted membrane vesicles was energized by a valinomycin (2 μM)-induced potassium diffusion potential ($\Delta\psi$) (100 mV) applied in the absence of a ΔpNa^+ at 40°C (▲). ○, no valinomycin addition. (B) Effect of CCCP (20 μM) (○) or DCCD (50 μM) (△) on ATP synthesis of inverted membrane vesicles energized by a valinomycin-induced potassium diffusion potential applied in the absence of ΔpNa^+ at 40°C (▲). All inhibitors were preincubated with the inverted membrane vesicles for 10 min prior to the addition of valinomycin. (C) Ability of an artificially imposed ΔpNa^+ (100 mV) to drive ATP synthesis in the presence of a valinomycin-induced potassium diffusion potential ($\Delta\psi$, 100 mV) (▲). The experiment was also performed with 5 μM monensin included in the reaction buffer (□). (D) Effect of CCCP (20 μM) on ATP synthesis in the presence of either a ΔpNa^+ and $\Delta\psi$ (▲) or $\Delta\psi$ alone (○). ATP synthesis was measured as described in Materials and Methods. For all experiments the values are the means of two to four independent determinations, and the associated experimental error was less than 15%.

Nine open reading frames were identified within the 7.2-kb region sequenced. These genes were organized in the order *atpIBEFHAGDC* and encode the *C. paradoxum* ATP synthase subunits *i*, *a*, *c*, *b*, δ, α, γ, β, and ε, respectively. This arrangement is identical to that of the *atp* operons from *E. coli* and other *Clostridium* species. The start codon of each gene was designated by alignment of *atp* gene sequences with those of other bacteria and the positions of potential ribosome-binding sites. Eight of the nine genes began with the typical ATG start codon, whereas the rare TTG codon is proposed for *atpI*. A putative transcription terminator was located immediately downstream from *atpC* (data not shown).

Properties of the predicted proteins. The calculated molecular masses of the nine ATP synthase subunits, as deduced

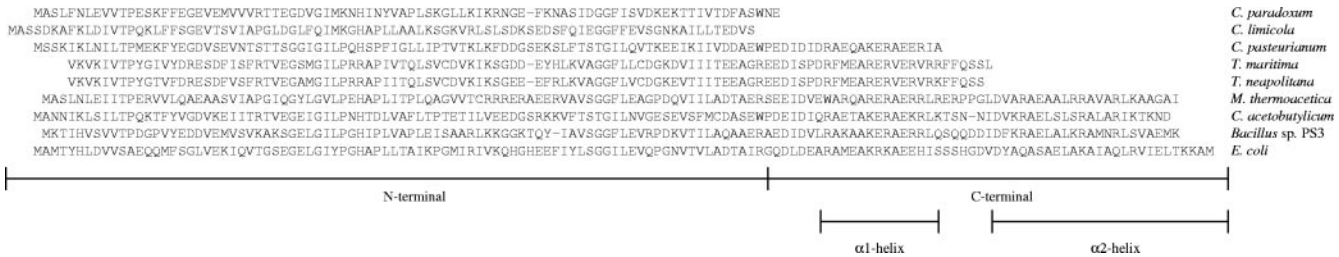

FIG. 7. Alignment of the ε subunits from *Chlorobium limicola* (58), *C. pasteurianum* (accession number AF283808), *Thermotoga maritima* (accession number AE001805), *Thermotoga neapolitana* (accession number AB004784), *M. thermoacetica* (accession number U64318), *C. acetobutylicum* (accession number AF101055), *Bacillus* sp. strain PS3 (accession number X07804), and *E. coli* (accession number J01594). The N-terminal part (residues 1 to 86) in *E. coli* and the C-terminal domain (residues 91 to 138) that is comprised of two antiparallel α-helices are indicated.

from the DNA sequence, were as follows: 14,184 Da (*i* subunit), 25,447 Da (*a* subunit), 8,255 Da (*c* subunit), 19,443 Da (*b* subunit), 20,763 Da (δ subunit), 55,667 Da (α subunit), 31,709 Da (γ subunit), 50,453 Da (β subunit), and 9,668 Da (ε subunit). These molecular masses corresponded well with the sizes obtained from the purified complex (Fig. 2). Although the structural gene encoding for subunit *i* was present in the *atp* operon of *C. paradoxum*, this subunit could not be purified along with the F_1F_o complex. A similar finding has been reported for other bacteria (4, 8, 12, 42).

The ε subunit from the *E. coli* F_1F_o-ATP synthase is a two-domain protein which consists of an N-terminal part that forms a 10-stranded β-sandwich structure (residues 1 to 86) and a C-terminal domain (residues 91 to 138) that forms two α-helices running antiparallel to one another (57). Alignment of the ε subunit from the *C. paradoxum* ATPase to those from other bacteria and *E. coli* (Fig. 7) revealed that, like the ε subunit from the green photosynthetic bacterium *Chlorobium limicola*, it lacks the entire C-terminal domain.

The deduced amino acid sequences for the α, β, and *c* subunits of the *C. paradoxum* ATP synthase were more conserved (between 65% and 83% identical residues) than those for the remaining six subunits (between 28% and 53% identical residues), compared to the corresponding subunits from other bacterial ATP synthases. Several motifs and residues in these three conserved subunits were evident. The α and β subunits contained the consensus nucleotide-binding domains Walker motifs A (GXXXXGKT) and B (L-hydrophobic-hydrophobic-hydrophobic-D) (1, 55) (data not shown), and the C-terminal domain of the β subunit contained the well-conserved acidic cluster sequence known as the DELSEED motif (^{385}DELS DED^{391} in *C. paradoxum*). In the *c* subunit, the polar loop (residues ^{41}KQPE^{44}) that connects the two hydrophobic α helices is present, as is the conserved DCCD-binding glutamate residue (E^{61}) in the center of the second transmembrane helix (Fig. 8).

Alignment of the *c* subunit to those from other bacteria (Fig. 8) showed stronger overall homology with Na^+-translocating F_1F_o-ATP synthases from *A. woodii* (83% identity), *P. modestum* (67% identity), and *I. tartaricus* (70% identity) than with the proton-coupled *E. coli* counterpart (27% identity) or those from other clostridia (42 to 50% identity). Furthermore, the Na^+-binding motif consisting of Q^{28}, E^{61}, and S^{62} (21, 37, 39, 45) was present in the *c* subunit of the *C. paradoxum* ATP synthase.

DISCUSSION

C. paradoxum is an anaerobic thermoalkaliphilic isolate that grows rapidly under conditions where the proton gradient for driving membrane-bound energetic processes appears to be suboptimal for growth (5). To study such energetic processes in *C. paradoxum*, we have conducted a biochemical and molecular characterization of the membrane-bound F_1F_o-ATP synthase. The results demonstrate that the ATP synthase from *C. paradoxum* is a Na^+-translocating F_1F_o-ATPase, the first reported for an alkaliphilic bacterium. The properties that define the enzyme as a Na^+-translocating F-type ATPase are as follows: ATP hydrolysis activity of the purified complex was stimulated in the presence of low concentrations of Na^+ ions, Na^+ ions provided protection against DCCD inhibition in a pH-dependent manner, and ATP synthesis in inverted membrane vesicles was observed in the presence of an artificially imposed ΔpNa^+ and $\Delta\psi$ that was sensitive to the sodium ionophore

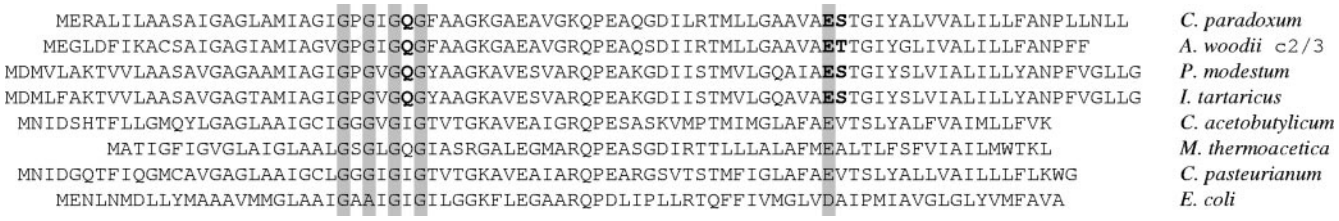

FIG. 8. Alignment of the *c* subunits from *A. woodii* (accession number U10505), *P. modestum* (accession number X53960), *I. tartaricus* (accession number AF522463), *C. acetobutylicum* (accession number AF101055), *M. thermoacetica* (accession number U64318), *C. pasteurianum* (accession number AF283808), and *E. coli* (accession number J01594). Conserved residues are shaded, and Na^+-binding residues are shown in boldface.

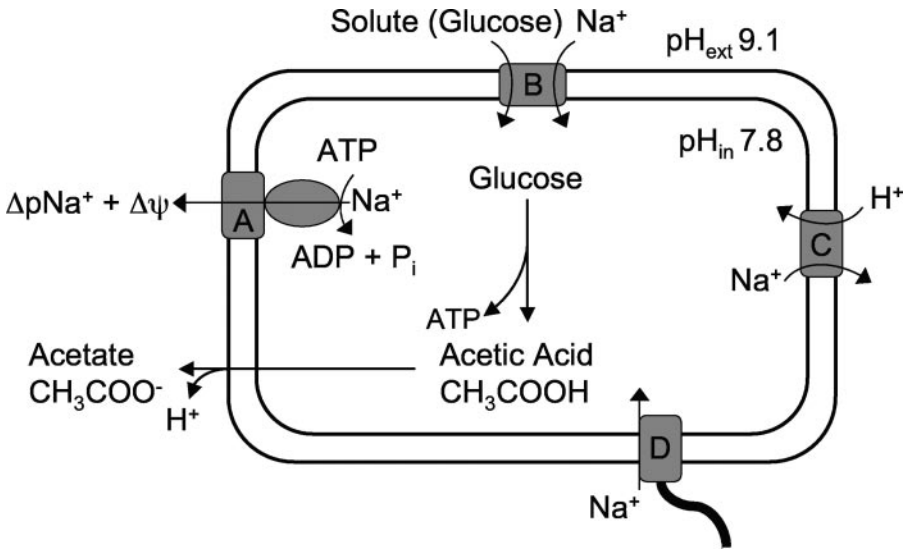

FIG. 9. Schematic diagram outlining the role of the Na^+-translocating F_1F_o-ATPase in membrane-bound bioenergetic processes of *C. paradoxum*. Proteins shown are as follows: A, Na^+-translocating ATPase; B, Na^+/solute symporter; C, Na^+/H^+ antiporter; D, flagellar rotor.

monensin. Further corroboration was provided by the cloning and subsequent DNA sequencing of the *C. paradoxum atp* operon, which revealed that the enzyme harbored the conserved Na^+-binding motif in the membrane-bound *c* subunit (viz., Q^{28}, E^{61}, and S^{62}). Validation of this sodium signature was the observed stable oligomeric *c*-ring on SDS-polyacrylamide gels and the conversion of this oligomer to its monomeric form by TCA treatment of the *C. paradoxum* ATPase.

To date, only three ATP synthases have been characterized from alkaliphilic bacteria, all of which are aerobic bacilli (4, 14, 15). The ATP synthases from these bacteria are proton coupled, work predominantly in the ATP synthesis direction, and exhibit latent ATPase activity. Analysis of the *atp* operons that encode these ATP synthases has revealed the presence of amino acid residues or putative motifs that appear to be unique to alkaliphilic bacilli (19, 20, 22). For example, the *a* subunit of alkaliphilic bacilli contains a lysine residue (K^{180}), found in transmembrane helix IV, that has been shown to be obligatory for the growth of *Bacillus pseudofirmus* on nonfermentable carbon sources at alkaline pH (56). This residue has been proposed to have a gating function implicated in the retention of protons at high pH. This lysine residue is not conserved in the *a* subunit of *C. paradoxum*, supporting the contention that this ATPase is not specifically adapted to capture protons at high pH but instead has a preference for Na^+ ions. This is further reinforced by the specific protection of DCCD inhibition of ATPase activity by Na^+ ions.

A notable feature of the ATPase from *C. paradoxum* is the complete absence of the C-terminal domain (two antiparallel α-helices) of the ε subunit, compared to the *E. coli* ε subunit. This appears to be unusual in light of recent single-molecule analysis of ATP synthesis and hydrolysis that demonstrates unequivocally that the ε subunit (from thermophilic *Bacillus* sp. strain PS3) is indispensable for coupled ATP synthesis but dispensable for ATP hydrolysis activity (47). Other studies have also proposed a role for the ε subunit in coupling rotation to ATP synthesis (3). On the basis of these findings, we propose that the ATP synthase of *C. paradoxum* is most likely geared in the ATP hydrolysis direction and potentially is never used to synthesize ATP. This is further substantiated by two observations: (i) very low rates of ATP synthesis are measured in membranes and the levels would appear to be too low to sustain a doubling time of 16 min at pH 9.8, and (ii) the metabolic pathway of *C. paradoxum* does not appear to contain a mechanism for generating either a ΔpNa^+ or $\Delta\psi$, which are required to fuel the ATP synthase. The bulk of ATP synthesized in *C. paradoxum* is thus generated by substrate-level phosphorylation (i.e., via phosphoglycerate kinase, pyruvate kinase, and acetate kinase), and the high growth rates achieved are the result of fast glycolytic flux through the fermentative pathway. Any excess ATP (i.e., above that required for driving catabolic and anabolic reactions in the cell) generated in this pathway could be hydrolyzed rapidly via the ATPase. Given the proposed role of ε, and particularly the C-terminal domain, in regulating potentially wasteful ATP hydrolysis activity, the regulation of ATPase activity warrants further investigation in anaerobic bacteria where other variations in the size of the C-terminal arm have been observed (7, 18, 58).

A model for the role of the F_1F_o-ATPase in the bioenergetics of *C. paradoxum* is presented in Fig. 9. Growth of *C. paradoxum* is sensitive to the electroneutral Na^+/H^+ antiporter monensin (5), suggesting that a ΔpNa^+ is obligatory for growth of this bacterium. The ATPase plays an important role in establishing the ΔpNa^+, fuelled by ATP that is rapidly produced from glycolysis (i.e., glucose is converted to acetate). The result of sodium pumping also leads to the formation of a $\Delta\psi$ (100 mV), which contributes to the overall electrochemical gradient of sodium ions ($\Delta\mu Na^+$). This is vitally important because many processes are obligatorily coupled to the $\Delta\psi$ component of the total $\Delta\mu Na^+$. While it remains to be experimentally proven, we propose that a ΔpNa^+ is used to drive both solute transport and motility, as observed for other alkaliphilic bacteria (28). Solute uptake and motility would also appear to serve as the major routes of sodium reentry (Fig. 9).

Further evidence for this hypothesis comes from studies with the anaerobic thermoalkaliphile *Anaerobranca gottschalkii*, where amino acid transport occurs in symport with Na^+ ions (44). Those authors also reported the presence of Na^+-stimulated ATPase activity in *A. gottschalkii* membrane vesicles, but this property was not examined further. The concept of a bacterium being exclusively coupled to Na^+ ions is exemplified in *Clostridium fervidus*, where all secondary transport systems utilize a $\Delta\mu Na^+$ generated by a V-type ATPase (17, 49, 50). For a thermophilic bacterium, the consequence of utilizing Na^+ ions over protons provides a bioenergetic advantage, as Na^+ ions are about 1,000-fold less membrane permeative than protons (53). In a proton desert (alkaline pH), the advantage of using Na^+ ions over protons is further magnified.

In aerobic (nonfermentative) alkaliphilic bacilli, a proton gradient is established by respiration, and through secondary Na^+/H^+ antiporters this proton gradient is used to regulate internal pH (i.e., acidify the cytoplasm) and generate a ΔpNa^+ for solute uptake and motility (28). It is presently not known how *C. paradoxum* maintains the cytoplasm at a near-neutral pH range when growing at high external pH. However, it should be mentioned that the magnitude of the ΔpH generated by *C. paradoxum* is much smaller (1.3 pH units) and over a narrower pH range (5) than those of aerobic alkaliphiles, which maintain a ΔpH of 1.9 to 2.5 pH units (acidic inside) over a broad pH range (16, 52). The role of a Na^+/H^+ antiporter in intracellular pH regulation by *C. paradoxum* remains to be determined, but the operation of such an exchanger powered by $\Delta\psi$ would need to be congruent with Na^+-pumping activity of the F_1F_o-ATPase as they will both compete for intracellular Na^+ ions (Fig. 9). The intracellular acetic acid (or other acids) produced from glucose metabolism by *C. paradoxum* will move rapidly across the cytoplasmic membrane (undissociated) and accumulate as acetate and protons in the alkaline exterior according to the Henderson-Hasselbalch equation (Fig. 9). This would be largely counterproductive for pH regulation at high pH, but the protons released in this reaction could be utilized by a Na^+/H^+ antiporter, thus potentially facilitating pH homeostasis.

In conclusion, our data demonstrate that the F_1F_o-ATPase from *C. paradoxum* plays a central role in growth at high pH and temperature. The enzyme offers further opportunities to understand how it has evolved to function as a hydrolytic motor with an apparent lack of ε subunit-mediated regulation under anaerobic conditions. Current studies are aimed at determining how this important enzyme is regulated.

ACKNOWLEDGMENTS

We express our appreciation to Ralph Jack for helpful discussions with regard to the purification of the ATPase, to Thomas Meier for expert technical advice and continued guidance pertaining to the *c*-oligomer purification, and to Sieu Tran for critical reading of the manuscript.

This work and S.K. were supported by a Marsden Grant from the Royal Society of New Zealand. S.A.F. was supported by an Otago Postgraduate Scholarship from the University of Otago.

REFERENCES

1. **Abrahams, J. P., A. G. W. Leslie, R. Lutter, and J. E. Walker.** 1994. Structure at 2.8 Å resolution of F_1-ATPase from bovine heart mitochondria. Nature **370:**621–628.
2. **Church, G. M., and W. Gilbert.** 1984. Genomic sequencing. Proc. Natl. Acad. Sci. USA **81:**1991–1995.
3. **Cipriano, D. J., and S. D. Dunn.** 2006. The role of the ε subunit in the *Escherichia coli* ATP synthase. The C-terminal domain is required for efficient energy coupling. J. Biol. Chem. **281:**501–507.
4. **Cook, G. M., S. Keis, H. W. Morgan, C. von Ballmoos, U. Matthey, G. Kaim, and P. Dimroth.** 2003. Purification and biochemical characterization of the F_1F_o-ATP synthase from thermoalkaliphilic *Bacillus* sp. strain TA2.A1. J. Bacteriol. **185:**4442–4449.
5. **Cook, G. M., J. B. Russell, A. Reichert, and J. Wiegel.** 1996. The intracellular pH of *Clostridium paradoxum*, an anaerobic, alkaliphilic, and thermophilic bacterium. Appl. Environ. Microbiol. **62:**4576–4579.
6. **Cotter, P. D., and C. Hill.** 2003. Surviving the acid test: responses of gram-positive bacteria to low pH. Microbiol. Mol. Biol. Rev. **67:**429–453.
7. **Das, A., and L. G. Ljungdahl.** 2003. *Clostridium pasteurianum* F_1F_o ATP synthase: operon, composition, and some properties. J. Bacteriol. **185:**5527–5535.
8. **Deckers-Hebestreit, G., and K. Altendorf.** 1996. The F_oF_1-type ATP synthases of bacteria: structure and function of the F_o complex. Annu. Rev. Microbiol. **50:**791–824.
9. **Dimroth, P., and G. M. Cook.** 2004. Bacterial Na^+- or H^+-coupled ATP synthases operating at low electrochemical potential. Adv. Microb. Physiol. **49:**175–218.
10. **Dimroth, P., C. von Ballmoos, T. Meier, and G. Kaim.** 2003. Electrical power fuels rotary ATP synthase. Structure **11:**1469–1473.
11. **Dmitriev, O. Y., P. C. Jones, and R. H. Fillingame.** 1999. Structure of the subunit *c* oligomer in the F_1F_o ATP synthase: model derived from solution structure of the monomer and cross-linking in the native enzyme. Proc. Natl. Acad. Sci. USA **96:**7785–7790.
12. **Futai, M., and H. Kanazawa.** 1983. Structure and function of proton-translocating adenosine triphosphatase (F_oF_1): biochemical and molecular biological approaches. Microbiol. Rev. **47:**285–312.
13. **Hanahan, D., J. Jessee, and F. R. Bloom.** 1991. Plasmid transformation of *Escherichia coli* and other bacteria. Methods Enzymol. **204:**63–113.
14. **Hicks, D. B., and T. A. Krulwich.** 1990. Purification and reconstitution of the F_1F_o-ATP synthase from alkaliphilic *Bacillus firmus* OF4. Evidence that the enzyme translocates H^+ but not Na^+. J. Biol. Chem. **265:**20547–20554.
15. **Hoffmann, A., and P. Dimroth.** 1991. The ATPase of *Bacillus alcalophilus*. Reconstitution of energy-transducing functions. Eur. J. Biochem. **196:**493–497.
16. **Hoffmann, A., and P. Dimroth.** 1991. The electrochemical proton potential of *Bacillus alcalophilus*. Eur. J. Biochem. **201:**467–473.
17. **Höner zu Bentrup, K., T. Ubbink-Kok, J. S. Lolkema, and W. N. Konings.** 1997. An Na^+-pumping V_1V_o-ATPase complex in the thermophilic bacterium *Clostridium fervidus*. J. Bacteriol. **179:**1274–1279.
18. **Iida, T., K. Inatomi, Y. Kamagata, and T. Maruyama.** 2002. F- and V-type ATPases in the hyperthermophilic bacterium *Thermotoga neapolitana*. Extremophiles **6:**369–375.
19. **Ivey, D. M., and T. A. Krulwich.** 1991. Organization and nucleotide sequence of the *atp* genes encoding the ATP synthase from alkaliphilic *Bacillus firmus* OF4. Mol. Gen. Genet. **229:**292–300.
20. **Ivey, D. M., and T. A. Krulwich.** 1992. Two unrelated alkaliphilic *Bacillus* species possess identical deviations in sequence from those of other prokaryotes in regions of F_o proposed to be involved in proton translocation through the ATP synthase. Res. Microbiol. **143:**467–470.
21. **Kaim, G., F. Wehrle, U. Gerike, and P. Dimroth.** 1997. Molecular basis for the coupling ion selectivity of F_1F_o ATP synthases: probing the liganding groups for Na^+ and Li^+ in the c subunit of the ATP synthase from *Propionigenium modestum*. Biochemistry **36:**9185–9194.
22. **Keis, S., G. Kaim, P. Dimroth, and G. M. Cook.** 2004. Cloning and molecular characterization of the *atp* operon encoding for the F_1F_o-ATP synthase from a thermoalkaliphilic *Bacillus* sp. strain TA2.A1. Biochim. Biophys. Acta **1676:**112–117.
23. **Keis, S., J. T. Sullivan, and D. T. Jones.** 2001. Physical and genetic map of the *Clostridium saccharobutylicum* (formerly *Clostridium acetobutylicum*) NCP 262 chromosome. Microbiology **147:**1909–1922.
24. **Kluge, C., and P. Dimroth.** 1993. Specific protection by Na^+ or Li^+ of the F_1F_o-ATPase of *Propionigenium modestum* from the reaction with dicyclohexylcarbodiimide. J. Biol. Chem. **268:**14557–14560.
25. **Knol, J., K. Sjollema, and B. Poolman.** 1998. Detergent-mediated reconstitution of membrane proteins. Biochemistry **37:**16410–16415.
26. **Kobayashi, H., and Y. Anraku.** 1972. Membrane-bound adenosine triphosphatase of *Escherichia coli*. J. Biochem. **71:**387–399.
27. **Krulwich, T. A.** 1995. Alkaliphiles: 'basic' molecular problems of pH tolerance and bioenergetics. Mol. Microbiol. **15:**403–410.
28. **Krulwich, T. A., M. Ito, R. Gilmour, D. B. Hicks, and A. A. Guffanti.** 1998. Energetics of alkaliphilic *Bacillus* species: physiology and molecules. Adv. Microb. Physiol. **40:**401–438.
29. **Laemmli, U. K.** 1970. Cleavage of structural proteins during the assembly of the head of bacteriophage T4. Nature **227:**680–685.
30. **Laubinger, W., and P. Dimroth.** 1988. Characterization of the ATP synthase of *Propionigenium modestum* as a primary sodium pump. Biochemistry **27:**7531–7537.
31. **Laubinger, W., and P. Dimroth.** 1987. Characterization of the Na^+-stimu-

lated ATPase of *Propionigenium modestum* as an enzyme of the F_1F_o type. Eur. J. Biochem. **168:**475–480.
32. **Laubinger, W., and P. Dimroth.** 1989. The sodium ion translocating adenosinetriphosphatase of *Propionigenium modestum* pumps protons at low sodium ion concentrations. Biochemistry **28:**7194–7198.
33. **Lerner, C. G., and M. Inouye.** 1990. Low copy number plasmids for regulated low-level expression of cloned genes in *Escherichia coli* with blue/white insert screening capability. Nucleic Acids Res. **18:**4631.
34. **Li, Y., L. Mandelco, and J. Wiegel.** 1993. Isolation and characterization of a moderately thermophilic anaerobic alkaliphile, *Clostridium paradoxum* sp. nov. Int. J. Syst. Bacteriol. **43:**450–460.
35. **Linnett, P. E., and R. B. Beechey.** 1979. Inhibitors of the ATP synthase system. Methods Enzymol. **55:**472–518.
36. **Matthey, U., G. Kaim, and P. Dimroth.** 1997. Subunit c from the sodium-ion-translocating F_1F_o-ATPase of *Propionigenium modestum*. Production, purification and properties of the protein in dodecylsulfate solution. Eur. J. Biochem. **247:**820–825.
37. **Meier, T., and P. Dimroth.** 2002. Intersubunit bridging by Na^+ ions as a rationale for the unusual stability of the c-rings of Na^+-translocating F_1F_o ATP synthases. EMBO Rep. **3:**1094–1098.
38. **Meier, T., U. Matthey, C. von Ballmoos, J. Vonck, T. Krug von Nidda, W. Kühlbrandt, and P. Dimroth.** 2003. Evidence for structural integrity in the undecameric c-rings isolated from sodium ATP synthases. J. Mol. Biol. **325:**389–397.
39. **Meier, T., P. Polzer, K. Diederichs, W. Welte, and P. Dimroth.** 2005. Structure of the rotor ring of F-type Na^+-ATPase from *Ilyobacter tartaricus*. Science **308:**659–662.
40. **Nesterenko, M. V., M. Tilley, and S. J. Upton.** 1994. A simple modification of Blum's silver stain method allows for 30 minute detection of proteins in polyacrylamide gels. J. Biochem. Biophys. Methods **28:**239–242.
41. **Neumann, S., U. Matthey, G. Kaim, and P. Dimroth.** 1998. Purification and properties of the F_1F_o ATPase of *Ilyobacter tartaricus*, a sodium ion pump. J. Bacteriol. **180:**3312–3316.
42. **Ohta, S., M. Yohda, M. Ishizuka, H. Hirata, T. Hamamoto, Y. Otawara-Hamamoto, K. Matsuda, and Y. Kagawa.** 1988. Sequence and over-expression of subunits of adenosine triphosphate synthase in thermophilic bacterium PS3. Biochim. Biophys. Acta **933:**141–155.
43. **Peddie, C. J., G. M. Cook, and H. W. Morgan.** 1999. Sodium-dependent glutamate uptake by an alkaliphilic, thermophilic *Bacillus* strain, TA2.A1. J. Bacteriol. **181:**3172–3177.
44. **Prowe, S. G., J. L. C. M. van de Vossenberg, A. J. M. Driessen, G. Antranikian, and W. N. Konings.** 1996. Sodium-coupled energy transduction in the newly isolated thermoalkaliphilic strain LBS3. J. Bacteriol. **178:**4099–4104.
45. **Rahlfs, S., and V. Müller.** 1997. Sequence of subunit *c* of the Na^+-translocating F_1F_o ATPase of *Acetobacterium woodii*: proposal for determinants of Na^+ specificity as revealed by sequence comparisons. FEBS Lett. **404:**269–271.
46. **Reidlinger, J., and V. Müller.** 1994. Purification of ATP synthase from *Acetobacterium woodii* and identification as a Na^+-translocating F_1F_o-type enzyme. Eur. J. Biochem. **223:**275–283.
47. **Rondelez, Y., G. Tresset, T. Nakashima, Y. Kato-Yamada, H. Fujita, S. Takeuchi, and H. Noji.** 2005. Highly coupled ATP synthesis by F_1-ATPase single molecules. Nature **433:**773–777.
48. **Senior, A. E., S. Nadanaciva, and J. Weber.** 2002. The molecular mechanism of ATP synthesis by F_1F_o-ATP synthase. Biochim. Biophys. Acta **1553:**188–211.
49. **Speelmans, G., B. Poolman, T. Abee, and W. N. Konings.** 1993. Energy transduction in the thermophilic anaerobic bacterium *Clostridium fervidus* is exclusively coupled to sodium ions. Proc. Natl. Acad. Sci. USA **90:**7975–7979.
50. **Speelmans, G., B. Poolman, and W. N. Konings.** 1993. Amino acid transport in the thermophilic anaerobe *Clostridium fervidus* is driven by an electrochemical sodium gradient. J. Bacteriol. **175:**2060–2066.
51. **Spruth, M., J. Reidlinger, and V. Müller.** 1995. Sodium-ion dependence of inhibition of the Na^+-translocating F_1F_o-ATPase from *Acetobacterium woodii*—probing the site(s) involved in ion-transport. Biochim. Biophys. Acta **1229:**96–102.
52. **Sturr, M. G., A. A. Guffanti, and T. A. Krulwich.** 1994. Growth and bioenergetics of alkaliphilic *Bacillus firmus* OF4 in continuous culture at high pH. J. Bacteriol. **176:**3111–3116.
53. **van de Vossenberg, J. L. C. M., T. Ubbink-Kok, M. G. Elferink, A. J. M. Driessen, and W. N. Konings.** 1995. Ion permeability of the cytoplasmic membrane limits the maximum growth temperature of bacteria and archaea. Mol. Microbiol. **18:**925–932.
54. **von Ballmoos, C., Y. Appoldt, J. Brunner, T. Granier, A. Vasella, and P. Dimroth.** 2002. Membrane topography of the coupling ion binding site in Na^+-translocating F_1F_o ATP synthase. J. Biol. Chem. **277:**3504–3510.
55. **Walker, J. E., M. Saraste, M. J. Runswick, and N. J. Gay.** 1982. Distantly related sequences in the α- and β-subunits of ATP synthase, myosin, kinases and other ATP-requiring enzymes and a common nucleotide binding fold. EMBO J. **1:**945–951.
56. **Wang, Z., D. B. Hicks, A. A. Guffanti, K. Baldwin, and T. A. Krulwich.** 2004. Replacement of amino acid sequence features of a- and c-subunits of ATP synthases of alkaliphilic *Bacillus* with the *Bacillus* consensus sequence results in defective oxidative phosphorylation and non-fermentative growth at pH 10.5. J. Biol. Chem. **279:**26546–26554.
57. **Wilkens, S., F. W. Dahlquist, L. P. McIntosh, L. W. Donaldson, and R. A. Capaldi.** 1995. Structural features of the ε subunit of the *Escherichia coli* ATP synthase determined by NMR spectroscopy. Nat. Struct. Biol. **2:**961–967.
58. **Xie, D.-L., H. Lill, G. Hauska, M. Maeda, M. Futai, and N. Nelson.** 1993. The *atp2* operon of the green bacterium *Chlorobium limicola*. Biochim. Biophys. Acta **1172:**267–273.
59. **Yanisch-Perron, C., J. Vieira, and J. Messing.** 1985. Improved M13 phage cloning vectors and host strains: nucleotide sequences of the M13mp18 and pUC19 vectors. Gene **33:**103–119.